DOI: 10.1002/anie.200801985

Electronic Structure

Calcium d States: Chemical Bonding of CaC_6

Shuiquan Deng, Arndt Simon, and Jürgen Köhler*

The recent discovery of massless Dirac fermions in single layers of graphite (graphene)[1] and superconductivity in graphite intercalation compounds (GICs) such as CaC_6 at unexpectedly high temperatures[2] stimulated intensive research to explore the nature and interactions of charge carriers in these low-dimensional systems. The early prediction of free-electron-like interlayer electronic states in graphite and the importance of the interlayer states for the formation of GICs,[3] verified experimentally,[4] are regaining considerable interest. Based on calculations on the structure of YbC_6 Csányi et al.[5] also characterized a similar quasi-free electron band in GIC and argued about its relevance for superconductivity. However, the proposed quasi-free-electron picture and the implied pairing mechanism are at odds with experiments,[6] particularly the large Ca isotope effect.[7] Mazin correctly predicted the interlayer band in CaC_6 as originating from calcium,[8a] but the chemical bonding remains unresolved. Recent theoretical work[8b] based on the correct structure of CaC_6 does not address the nature of chemical bonding. Here we report our studies on CaC_6 using the full-potential linear muffin-tin orbital (FP-LMTO) method,[9] semi-empirical extended Hückel (EH) method,[10] and the tight-binding (TB) model.

Figure 1 shows the $R\bar{3}m$ rhombohedral structure of CaC_6. The structure exhibits AaAbAcAa… stacking of graphene sheets (A) and metal-atom layers (a, b, c) in such a way that the metal atoms center the hexagons of the graphene sheets. In contrast, the structure of YbC_6, which contains analogous graphene and metal-atom layers, has the stacking sequence AaAbAa…

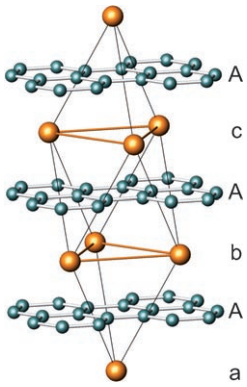

Figure 1. Crystal structure of CaC_6, where a, b, c indicate the different packing patterns of the Ca layers relative to the graphene sheets (A).

[*] Dr. S. Deng, Prof. Dr. A. Simon, Prof. Dr. J. Köhler
Max-Planck-Institut für Festkörperforschung
Heisenbergstrasse 1, 70569 Stuttgart (Germany)
Fax: (+49) 711-689-1091
E-mail: s.deng@fkf.mpg.de

Our first-principles FP-LMTO calculations for CaC_6[11] resulted in C 2s and $2p_\sigma$ bands far below the Fermi energy, as expected. The Ca valence bands lie close to the Fermi level. The calculated band structure along four symmetry lines together with the total density of states (DOS) and four partial DOSs are shown in Figure 2.

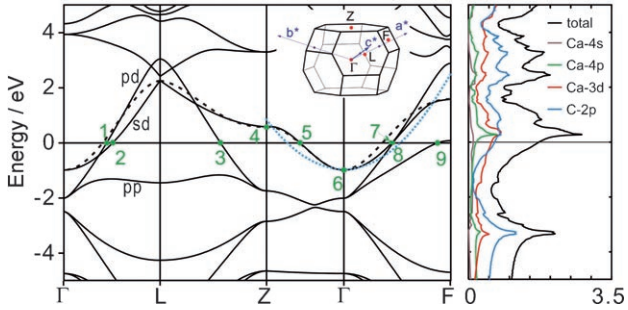

Figure 2. Band structure together with the first Brillouin zone and DOS curves for CaC_6, calculated with the FP-LMTO method. The broken curve is the tight-binding band from our TB model. The blue dotted line is the energy dispersion of quasi-free electrons along two different directions. The three bands crossing the Fermi level are named pp, sd, and pd, respectively, with relevant states (green dots) around the Fermi level numbered from left to right.

Three bands, pp, sd, and pd in the order of their energies, cross the Fermi level. The assignments follow the calculated orbital compositions[12] for some representative states Ψ at and around the Fermi level, indicated by dots in Figure 2. According to the compositions of Ψ at points 1, 3, and 8 the pd band is dominated by C p_z with a small admixture of Ca d of e_g symmetry. The pp band represented by point 9 is dominated by C p_z with a small contribution from Ca p_z. In fact, among the investigated states, $\Psi(9)$ is the only one that contains Ca p to which the high energy is attributed, as indicated by the calculated potential parameters of $C_\nu = 23.360$, 28.664, and 30.962 eV for the Ca 4s, 3d, and 4p canonical band centers,[13] respectively. The sd band represented by points 2, 4, 5, 6, and 7 is the most interesting, because it has nearly pure Ca character derived from its 4s3d hybrid without any significant contribution from the graphene layer. In the earlier study quasi-free-electron behavior was assigned to this band.[5] However, as a plane-wave basis set, which does not depend on atoms present, was used with the pseudopotential method, any assignment of the band character must be done with care.

Our FP-LMTO calculations characterize the selected states around the Fermi level in more detail than the previous LAPW calculations.[8a] To further clarify the nature of the sd band an analytic tight-binding dispersion relation $E(\boldsymbol{k})$ along different symmetry directions was derived.[14] The result is drawn in Figure 2 as a broken line. The agreement with the

FP-LMTO band is reasonably good, which indicates that the sd band is based on a tight-binding orbital centered at Ca rather than quasi-free electrons. For comparison, the quasi-free electron band calculated according to $E(\boldsymbol{k}) = \boldsymbol{k}^2 + V(0)$ is shown as a blue dotted line by setting the potential $V(0)$ to the appropriate energy at Γ.[15]

The tight-binding character of the sd band is evident from the above analysis, and our FP-LMTO calculations indicated the significance of the Ca d states in producing it. The surprising action of calcium as a d metal needs further elucidation. To do so, we chose the extended Hückel (EH) method[10] because of its transparency and success in chemical bonding analysis. Whereas the default EH parameters of C could be used, changes to the default parameters and, in particular inclusion of the Ca 3d state, were necessary to produce the interlayer band. These parameters were optimized with the help of a combination of the golden selection rule[16] and the orthogonal array.[17]

The band structure of CaC_6 calculated with the optimized parameters[18] is shown in Figure 3. The sd band (red in Figure 3a) completely disappears when participation of the Ca d state is omitted (Figure 3b), in contrast to the pd and pp bands, which remain with only minor changes.

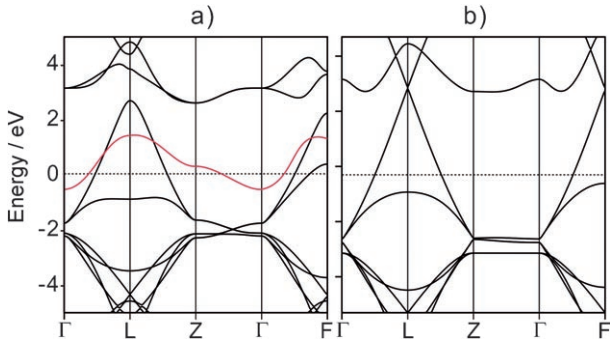

Figure 3. Extended Hückel band structures of CaC_6 calculated from our optimized parameters. a) With inclusion of Ca 3d states and b) without inclusion of Ca 3d states.

Comparing the ζ values of the third-row transition metal 3d orbitals[10b] reveals that the Ca 3d orbital is the least tightly binding. Interestingly, it is closest to the Yb 5d orbital, the sd hybrid of which in YbC_6 was determined by angle-resolved photoemission spectroscopy.[6a] As is also clear from Figure 3, the Ca 3d states of E_g symmetry modify the pd band but are not necessary to create it. The presence of the Ca 3d state was also confirmed by recent theoretical work on JIG (jellium intercalated graphite).[19]

With the above facts established the question arises to what extent the Ca 3d state changes the total energy. Within the density functional framework,[20] the total energy functional of charge density ρ is a sum of kinetic, Coulomb and exchange-correlation terms $E[\rho] = T[\rho] + U[\rho] + E_{xc}[\rho]$. The changes of $T[\rho]$ and $E_{xc}[\rho]$ pose no problem in the FP-LMTO algorithm. However, much effort is needed to single out the contribution of a specific term[21] in $U[\rho]$ due to the use of, for example, multipole potentials in solving the Poisson equation,[9] because E_{ee}, E_{Ne}, E_{NN} (e: electron, N: nuclear) are all mixed. We found values of 10.54, −1.60, −16.25, and −7.32 eV cell^{-1} for ΔT, ΔE_{xc}, ΔU, and ΔE, respectively, by calculations with and without d orbitals. Hence, the Ca 3d state decreases the Coulomb energy and the exchange-correlation energies but increases the kinetic energy. However, for the Coulomb energy the values of ΔE_{ee} and ΔE_{Ne} are 22.90 and −39.16 eV cell^{-1}, respectively. Considering the fact that the nuclear field of Ca only favors the s state within its muffin-tin sphere, we can conclude that the Ca 3d state is stabilized by the nuclear field of the C atoms and the many-body exchange-correlation effect with a total energy gain of 7.32 eV cell^{-1}.

The topologies of several states around the Fermi level and their bonding properties are shown in Figure 4. The sd hybrid shown in Figure 4a has a lower energy than that in Figure 4b, because the former has a dominant s component, while the latter has a dominant d component. The chemical bonding properties of these states are given by the (***k***-COHP) ***kj***-dependent bonding indicator[22] in the spirit of COHP.[23]

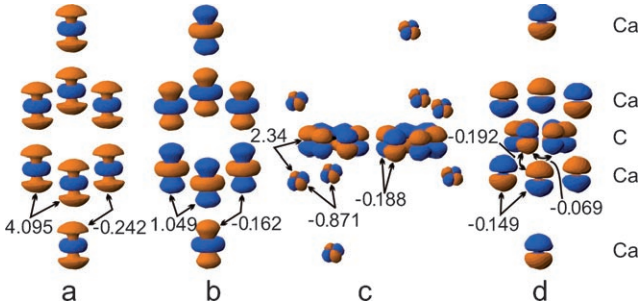

Figure 4. Orbital topologies of Fermi states in one unit cell (at slightly different angles of projection) together with ***k***-COHP values (×10^3 eV) a) at Γ for $\Psi(6)$, b) at Z for Ψ (4), c) real (left) and imaginary (right) part of $\Psi(1)$, and d) $\Psi(\mathbf{F})$, where the lobes of Ca $4p_z$ are magnified. The atoms in the rhombohedral unit cell are denoted.

As shown in Figure 4a and b, the intralayer antibonding interactions between the sd hybrids are one order of magnitude stronger than those of bonding interlayer interactions. As is clear from Figure 4, the indicated bonding and antibonding properties can not be directly assigned by simple inspection of the signs of the lobes of the involved hybrids. First of all, the bonding/antibonding interactions between different components of the hybrids may be different, as is obvious from Figure 4. Therefore the net bonding/antibonding property is decided by the major ones. The other reasons have already been given and discussed by Dronskowski and Blöchl.[23] The assignment of bonding/antibonding nature by inspection of the phases of the orbitals simply fails in the case of low-symmetry ***k*** points, because the real and imaginary parts may have very different phase structures, as can be seen in Figure 4c. The major interaction for $\Psi(1)$ and $\Psi(\mathbf{F})$ is the antibonding Ca–C interaction, though the former is one order of magnitude larger than the latter. However for $\Psi(\mathbf{F})$, the intralayer Ca–Ca interaction is just a little smaller than the Ca–C interaction. As can be seen from the ***k***-COHP values in Figure 4, all of the studied states are of antibonding type. The

dominant intralayer Ca–Ca and Ca–C interactions imply the importance of Ca vibrations, which gives a chemical-bonding explanation for the isotope effect.

In Figure 5, bonding between the Ca atoms within one layer in CaC_6 for the energy range of ± 0.9 eV around the Fermi level is visualized by the electron localization function

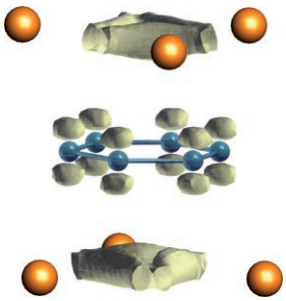

Figure 5. Isosurface of ELF around the Ca and C atoms in CaC_6, calculated in the energy range of ± 1.17 eV around the Fermi level and plotted with an isosurface value of 0.7.

(ELF)[24] calculated by the ab initio TB-LMTO method.[25] The bonding attractor lies within the triangle of the Ca atoms and the analogy to a three-center, two-electron bond is obvious. This situation is also similar to what has been found for transition metal dichalcogenides, which are known as charge-density wave materials,[26] and reflects the tendency of the Ca atoms in CaC_6 to behave more as an sd metal rather than an s or sp metal. It will be of interest to further study its consequence in some other GIC systems and Ca-containing compounds.[27]

In summary, our model and first-principle studies have demonstrated that in CaC_6 the Ca 3d state is a necessary and sufficient condition to produce the interlayer band. Significant occupation of d states is also essential for understanding the chemical bonding in elemental Ca.[28] The interlayer band in CaC_6 was found to be important to superconductivity in GIC, but incorrectly considered as a free-electron band.[5] The deep involvement of the Ca 3d states in the chemical bonding of the sd and pd band and particularly its tight-binding character explain the unusual Ca isotope effect. The C ligand field and the exchange-correlation effect have been shown to stabilize the Ca 3d states. The band structure of CaC_6 also shows a flat/steep band feature[29] characteristic of a superconductor. The analysis along this line and studies into the dynamic properties of CaC_6 are in progress.

Received: April 28, 2008
Published online: July 21, 2008

Keywords: ab initio calculations · calcium · carbon · electronic structure · intercalations

[1] a) K. S. Novoselov, A. K. Geim, S. V. Morozov, D. Jiang, M. I. Katsnelson, I. V. Grigorieva, S. V. Dubonos, A. A. Firsov, *Nature* **2005**, *438*, 197; b) A. Bostwick, T. Ohta, T. Seyller, K. Horn, E. Rotenberg, *Nat. Phys.* **2007**, *3*, 36.

[2] a) T. E. Weller, M. Ellerby, S. S. Saxena, R. P. Smith, A. N. T. Skipper, *Nat. Phys.* **2005**, *1*, 39; b) N. Emery, C. Hérold, M. d'Astuto, V. Garcia, C. Bellin, J. F. Marêché, P. Lagrange, G. Loupias, *Phys. Rev. Lett.* **2005**, *95*, 087003; c) N. Emery, C. Hérold, P. Lagrange, *J. Solid State Chem.* **2005**, *178*, 2947.

[3] M. Posternak, A. Baldereschi, A. J. Freeman, E. Wimmer, M. Weinert, *Phys. Rev. Lett.* **1983**, *50*, 761.

[4] T. Fauster, F. J. Himpsel, J. E. Fischer, E. W. Plummer, *Phys. Rev. Lett.* **1983**, *51*, 430.

[5] G. Csányi, P. B. Littlewood, A. H. Nevidomskyy, C. J. Pickard, B. D. Simons, *Nat. Phys.* **2005**, *1*, 42.

[6] a) S. L. Molodtsov, C. Laubschat, M. Richter, Th. Gantz, A. M. Shikin, *Phys. Rev. B* **1996**, *53*, 16621; b) G. Lamura, M. Aurino, G. Gufariello, E. Di Gennaro, A. Andreone, N. Emery, C. Hérold, J. F. Marêché, P. Lagrange, *Phys. Rev. Lett.* **2006**, *96*, 107008; c) J. S. Kim, L. Boeri, R. K. Kremer, F. S. Razavi, *Phys. Rev. B* **2006**, *74*, 214513.

[7] D. G. Hinks, D. Rosenmann, H. Claus, M. S. Bailey, J. D. Jorgensen, *Phys. Rev. B* **2007**, *75*, 014509.

[8] a) I. I. Mazin, *Phys. Rev. Lett.* **2005**, *95*, 227001; b) M. Calandra, F. Mauri, *Phys. Rev. Lett.* **2005**, *95*, 237002.

[9] a) S. Y. Savrasov, *Phys. Rev. B* **1996**, *54*, 16470; b) F. Janak, V. L. Moruzzi, A. R. Williams, *Phys. Rev. B* **1975**, *12*, 1257; c) J. P. Perdew, Y. Wang, *Phys. Rev. B* **1992**, *45*, 13244.

[10] a) R. Hoffmann, *J. Chem. Phys.* **1963**, *39*, 1397; b) G. A. Landrum, YaeHMOP: Yet Another extended Hückel Molecular Orbital Package.

[11] The experimental structural data for CaC_6 from Ref. [2c] were used throughout this work. 2κ 4s, 4p, 3d and 2s, 2p basis sets for Ca and C, respectively, were used for the expansion of valence states, while the Ca 3s, 3p states were treated as semicore states. In the interstitial region, the pseudo-LMTOs were expanded in plane waves up to 75.64, 109.5, and 156.5 eV for the Ca 4s, 4p, and 3d shells, and 533.3, 776.8 eV for C 2s and 2p shells, respectively, while the potential and charge density in the interstitial region were expanded in plane waves up to 2250.9 eV, corresponding to 17752 plane waves. 4237 and 13 independent k points for the valence and semicore states, respectively, were used in the self-consistent calculations.

[12] Orbital compositions for some representative Fermi states: $\Psi(\mathrm{pd},1) = 15.1\,\%\ E_g\ (\mathrm{Ca\ d}_{xy} + \mathrm{Ca\ d}_{x^2-y^2}) + 14.7\,\%\ E_g\ (\mathrm{Ca\ d}_{xz} + \mathrm{Ca\ d}_{yz}) + 64.9\,\%\ A_{2u}\ \mathrm{C\ p}_z$; $\Psi(\mathrm{sd},2) = 60.9\,\%\ \mathrm{A_{1g}\ Ca\ s} + 15.6\,\%\ \mathrm{A_{1g}\ Ca\ d}_{z^2}$); $\Psi(\mathrm{pd},3) = 30.0\,\%\ \mathrm{E_g\ (Ca\ d}_{xz} + \mathrm{Ca\ d}_{yz}) + 68.9\,\%\ \mathrm{A_{2u}\ C\ p}_z$; $\Psi(\mathrm{sd},4) = 22.7\,\%\ \mathrm{A_{1g}\ Ca\ s} + 66.3\,\%\ \mathrm{A_{1g}\ Ca\ d}_{z^2}$); $\Psi(\mathrm{sd},5) = 37.1\,\%\ \mathrm{A_{1g}\ Ca\ s} + 51.2\,\%\ \mathrm{A_{1g}\ Ca\ d}_{z^2}$); $\Psi(\mathrm{sd},6) = 63.4\,\%\ \mathrm{A_{1g}\ Ca\ s} + 32.2\,\%\ \mathrm{A_{1g}\ Ca\ d}_{z^2}$; $\Psi(\mathrm{sd},7) = 49.9\,\%\ \mathrm{A_{1g}\ Ca\ s} + 23.9\,\%\ \mathrm{A_{1g}\ Ca\ d}_{z^2} + 11.3\,\%\ \mathrm{A_{2u}\ C\ p}_z$; $\Psi(\mathrm{pd},8) = 30.4\,\%\ \mathrm{E_g\ (Ca\ d}_{xy} + \mathrm{Ca\ d}_{x^2-y^2}) + 56.6\,\%\ \mathrm{A_{2u}\ C\ p}_z$; $\Psi(\mathrm{pp},9) = 15.5\,\%\ \mathrm{A_{2u}\ Ca\ p}_z + 77.3\,\%\ \mathrm{A_{2u}\ C\ p}_z$. The contributions below 10% are omitted for brevity. The orbitals are grouped according to their symmetry in the corresponding point group of $\bar{R}m$.

[13] O. K. Andersen, O. Jepsen, *Physica B* **1977**, *91*, 317.

[14] Tight-binding dispersion relation of the sd hybrid band: $E_{\Gamma\text{-}L}(x) = \alpha + 2\beta + 4\gamma + (4\beta + 2\gamma + 6\delta)\cos(2\pi x)$; $E_{L\text{-}Z}(x) = \alpha + 2\beta - 2\gamma - 4\delta + 4\beta\cos[(2x-1)\pi] + 4\gamma\cos(2\pi x) + 2\delta\cos[(4x-1)\pi]$; $E_{Z\text{-}\Gamma}(x) = \alpha + 6\beta + (6\gamma + 6\delta)\cos(2\pi x)$; $E_{\Gamma\text{-}F}(x) = \alpha + 2\beta + 2\gamma + 4\delta + (4\beta + 4\gamma)\ \cos(2\pi x) + 2\delta\cos(4\pi x)$, where α is the on-site energy of the sd hybrid, β, γ, δ are the hopping integrals for 1st , 2nd, and 3rd nearest neighbors for a sd hybrid, respectively, and x is a parameter ranging between 0 and $^1/_2$. In deriving the above formula, it is assumed that there is no hybridization between the sd hybrids and other states, and a cutoff for such interactions to the 3rd nearest neighbors is taken. Global fitting to the first-principles sd band was not attempted; instead, the parameters α, β, γ, δ are extracted with the eigenvalues at the special points Γ, L, Z, and F. The obtained values are 27.651, −0.2655, −0.0555, and −0.0747 eV for α, β, γ, δ, respectively.

[15] Simulation of free-electron behavior: The formula for the quasi-free electron $E = k^2 + V(0)$ is given in the Rydberg atomic unit. Along the Γ–Z direction, $k = \alpha(g_1+g_2+g_3)$, with $0 \le \alpha \le 1/2$, while along the Γ–F direction, $k = \alpha(g_1+g_2)$, with $0 \le \alpha \le 1/2$, where g_i are the reciprocal lattice vectors corresponding to the primitive basis vectors of the direct lattice. By choosing k in this way, the anisotropy of the structure is implicitly considered.
[16] R. A. Dunlap, *The Golden Ratio and Fibonacci Numbers*, World Scientific Publishing, Singapore, **1997**.
[17] A. S. Hedayat, N. J. A. Sloane, J. Stufken, *Orthogonal Arrays: Theory and Applications*, Springer, New York, **1999**.
[18] Optimized EH parameters for Ca in this work: H4s (eV): −9.5, ζs: 1.6; H4p: −2.5, ζp: 1.6, H3d: −7.0, ζ1,3d: 2.74, c1:0.413, ζ2,3d: 1.13, c2: 0.7228; standard parameters: H4s (eV): −7.0, ζs: 1.2; H4p: −4.0, ζp: 1.2.
[19] L. Boeri, G. B. Bachelet, M. Giantomassi, O. K. Andersen, *Phys. Rev. B* **2007**, *76*, 064510.
[20] P. Hohenberg, W. Kohn, *Phys. Rev. B* **1964**, *136*, 864.
[21] Terms contained in the Coulomb potential energy, where $Z_{\mathbf{R}}$ is the nuclear charge at $\mathbf{R}$, E_{ee} is the static Coulomb interaction between electrons, E_{Ne} is the nuclear electron interaction, and E_{NN} is the nuclear–nuclear interaction [$\Delta M = M[\rho]_{\text{with d}} - M[\rho]_{\text{without d}}$ ($M = E$, T, U, E_{xc},...)]:

$$U[\rho] = \frac{1}{2}\int\frac{\rho(\mathbf{r})\rho(\mathbf{r}')}{|\mathbf{r}-\mathbf{r}'|}d\mathbf{r}d\mathbf{r}' - \sum_{\mathbf{R}} Z_{\mathbf{R}}\int\frac{\rho(\mathbf{r})d\mathbf{r}}{|\mathbf{r}-\mathbf{R}|} + \frac{1}{2}\sum_{\mathbf{R}\neq\mathbf{R}'}\frac{Z_{\mathbf{R}}Z_{\mathbf{R}'}}{|\mathbf{R}-\mathbf{R}'|} = E_{ee} + E_{Ne} + E_{NN}$$

[22] S. Deng, A. Simon, J. Köhler, A. Bussmann-Holder, *J. Supercond.* **2003**, *16*, 919. In this work, the real-space hopping integrals and orbital coefficients are all extracted from FP-LMTO calculations.
[23] R. Dronskowski, P. E. Blöchl, *J. Phys. Chem.* **1993**, *97*, 8617.
[24] a) A. D. Becke, K. E. Edgecombe, *J. Chem. Phys.* **1990**, *92*, 5397; b) A. Savin, O. Jepsen, O. K. Andersen, H. Preuss, H. G. von Schnering, *Angew. Chem.* **1992**, *31*, 187; c) B. Silvi, A. Savin, *Nature* **1994**, *371*, 683.
[25] R. Tank, O. Jepsen, A. Burkhardt, O. K. Andersen, TB-LMTO-ASA (version 4.7) **1998**, MPI für Festkörperforschung, Stuttgart, Germany.
[26] a) K. A. Yee, T. Hughbanks, *Inorg. Chem.* **1991**, *30*, 2321; b) M.-H. Whangbo, E. Canadell, *J. Am. Chem. Soc.* **1992**, *114*, 9587.
[27] a) M. Springborg, R. C. Albers, *Synth. Met.* **1993**, *56*, 3383; b) C.-M. Fang, J. Bauer, J. Y. Saillard, J. F. Halet, *Z. Naturforsch. B* **2007**, *62*, 971.
[28] a) S. Deng, A. Simon, J. Köhler, *Solid State Sci.* **2000**, *2*, 31; b) J. P. Jan, H. L. Skriver, *J. Phys. F* **1981**, *11*, 805.
[29] a) A. Simon, *Angew. Chem.* **1997**, *109*, 1873; *Angew. Chem. Int. Ed. Engl.* **1997**, *36*, 1788; b) S. Deng, A. Simon, J. Köhler, *Struct. Bonding (Berlin)* **2005**, *114*, 103.

